Sens. & Instrumen. Food Qual. (2007) 1:169–175
DOI 10.1007/s11694-007-9019-8

ORIGINAL PAPER

Lime characterization as a food additive

Miguel Galvan-Ruiz · Leticia Baños · Mario E. Rodriguez-Garcia

Received: 23 April 2007 / Accepted: 6 August 2007 / Published online: 22 August 2007

Abstract This article discusses the use of various measurement techniques for physico-chemical and mineralogical analyze of lime for its safe use as a food additive. Two types of samples were taken from a mine in Queretaro, Mexico, and measurements were made to determine Pb (CaO—0.0012 mg/kg, $Ca(OH)_2$—0.0527 mg/kg), As (CaO—0.0290 mg/kg, $Ca(OH)_2$—0.0849 mg/kg), F (under the quantification limit), and V (CaO—1.9068 mg/kg, $Ca(OH)_2$—4.3403 mg/kg). The samples were within the safety limits for human consumption. It is suggested that similar analysis be carried out on commercially marketed lime products.

Keywords Calcium oxide · Calcium hydroxide · Food additive · Safety limits · Pollutants · Human consumption

M. Galvan-Ruiz (✉)
Facultad de Ingeniería, División de Estudios de Posgrado, Universidad Autónoma de Querétaro, Centro Universitario Cerro de las Campanas, Queretaro, Qro. 76010, Mexico
e-mail: miguel@fata.unam.mx

M. Galvan-Ruiz
Centro de Estudios Tecnológicos Industrial y de Servicios 105, Santa María Magdalena, Queretaro 76137, Mexico

L. Baños
Instituto de Investigaciones en Materiales, Universidad Nacional Autónoma de México, Ciudad Universitaria, Mexico, DF 04510, Mexico

M. E. Rodriguez-Garcia
Centro de Física Aplicada y Tecnología Avanzada, Departamento de Nanotecnologia, Universidad Nacional Autónoma de México Campus Juriquilla, A. P. 1-1010, Queretaro 76000, Mexico

Introduction

Calcium is the most abundant mineral in the human body. Nordin [1] reported that it is a fundamental nutrient present in a good number of metabolic processes and it provides rigidity to bones and teeth, where 99% of body calcium resides. Power et al. [2] claims that numerous diseases of human beings, including bone fragility, hypertension, and colon cancer may be caused by chronically low dietary calcium intake. According to Flynn [3], and Flynn and Cashman [4], there is considerable evidence supporting that increasing the calcium intake over average consumption may have benefits for the development and strengthening of bones, reducing the risk of osteoporosis in later life. Dietary habits need to be changed for increased calcium intake (Rennera et al. [5]). The findings of many of these controlled calcium intervention trials have been formerly reviewed (Prentice [6]).

According to the National Institutes of Health [7] and the Institute of Medicine [8], the best source of calcium is food. The optimal calcium intake varies from 400 to 1,500 mg/day. Calcium can be safely consumed up to 2,000 mg/day. Serna-Saldivar et al. [9, 10] established that the population of many countries consume less of the recommended calcium amount. In developing countries, like Mexico and Central America, calcium intake is frequently limited by the high cost of dairy products and lactose intolerance.

An example of calcium-enriched food is the Mexican and Mesoamerican tortilla. Rodriguez et al. [11, 12] showed that the calcium content in tortillas varies from 0.07 (endogenous content in corn kernels) to 0.5%. Consequently, this kind of food provides an important source of calcium for a daily diet. In addition, related nixtamalized products, such as snacks, nachos and tamales, have

contributed to an increase in the calcium intake of the population. Additional elemental calcium in tortillas and other nixtamalized products comes from the addition of lime (in the forms of CaO or $Ca(OH)_2$) during the nixtamalization process (Rooney et al. [13]). An increase of calcium in the daily diet is the most important benefit of nixtamalized products consumption. During the last four decades the nixtamalization process has been studied (Bressani et al. [14, 15], Cortés-Gómez et al. [16]). These studies were focused on the physico-chemical properties of instant corn flour, tortillas and snacks, but there has not been much discussion on mineral content and risky substances included in $Ca(OH_2)$, despite the fact that lime has been listed under the European Union Food Standards Agency [17] as an approved additives and the US Food and Drug Administration as a direct food substance (GRAS) [18].

The use of lime in the nixtamalization process increases the pH value of the cooking liquor from 7 to 12, allowing the pericarp removal and increases the final product calcium content (Fernández- Muñoz et al. [19, 20]).

Annual consumption of tortillas in Mexico is 120 kg per capita, or 328 g/day (Figueroa-Cárdenas et al. [21]). The nixtamalization process requires 11.5–13.5 g of lime per maize kg, thus 100,000 ton/year of lime is used exclusively for tortillas in Mexico according to the "Asociación Nacional de Fabricantes de Cal" database [22]. It is relevant to mention that in Mexico there is no control over the regulation of lime for human consumption. Therefore, there is a need for further study and analysis.

Lime is the result of a process where calcite is extracted and calcined in a kiln to produce CaO and then $Ca(OH)_2$, which is a dry powder obtained by adding water to CaO thereby transforming the oxides into hydroxides. Raw materials could have chemical impurities. Due to the calcination by fossil fuels and with the addition of water during hydratation, certain contaminants could be introduced.

This article discusses the physico-chemical and mineralogical changes produced during the lime manufacturing process by detecting the presence of pollutants, which constitute a public health risk. The structure of crystalline phases was studied with X-ray diffraction. Low vacuum scanning electron microscopy was used to obtain information related to the particles morphology, and complementary electron dispersive scanning was used for semi-quantitative chemical analyses. Atomic absorption spectroscopy, ion chromatography, and inductively coupled plasma-mass spectrometry were used for quantitative analyses. Infrared and micro-Raman spectroscopies were used to detect the presence of pollutants.

Materials and methods

Sampling

Samples of CaO and $Ca(OH)_2$ were obtained from a mine in Bernal, Queretaro, Mexico. Three samples of approximately equal weight, each sample with a minimum of 250 g from different positions were taken under standard procedures and carried out isolated in sealed plastic bags. The total samples were mixed and repeatedly quartered down providing a representative sample. The samples are described in Table 1. SA1 is CaO and SA2 is $Ca(OH)_2$. Initially, raw material was fed to a vertical shaft lime kiln for preheating and calcination between 900 and 1,200 °C, decomposing the $CaCO_3$ into CaO and CO_2. The material was cooled and transferred into a hammer mill for crushing. After this process SA1 was obtained. SA2 was obtained after the hydratation process during CaO slaking. When exposed to water, CaO shows a strong moisture affinity. A reaction occurs and heat is generated at the same time with expansive forces, producing a total collapse of the lime particles. Even though the presence of sulfur is not as significant as the quantity of other major pollutants, sulfur content in raw materials or added during the manufacturing process could represent a problem.

Methods

X-ray diffraction

The X-ray diffraction patterns of samples were recorded on a diffractometer (Siemens D5000) operating at 35 kV, 15 A, and a Cu Kα radiation wavelength of 1.5406 Å. The measurements were performed at room temperature from 4° to 70° on a 2θ scale and with a step size of 0.05°.

Low vacuum Scanning Electron microscopy (LV-SEM)

Micrographs and semi-quantitative analyses of the samples were done in a Low Vacuum Scanning Electron Microscope (LV-SEM) (Jeol LV-SEM JSM 5600LV, Japan), with a resolution of 5 nm in LV mode, coupled with an Energy Dispersive X-ray Spectrometer (EDS) (Noran instrument, model Voyager 4.2.3, USA). The equipment was set at 20 kV electron acceleration voltage and 12–20 Pa of pressure in the specimen chamber.

Atomic Absorption Spectroscopy (AAS)

The samples were prepared by the dry-ashing procedure 968.08 AOAC [23]. The quantitative analyses were made

Table 1 Lime samples in the forms of calcium oxide and calcium hydroxide

Sample	Source of sampling	Type	Active clay materials	Slaking time	Color	Condition
SA-1	Factory vertical kiln	Quick lime—obtained directly from kiln exit	<6%	Very fast	Whitish	Soft, light weight rock
SA-2	Factory warehouse	Slaked lime under NMX-C-005-1996-ONNCCE specifications (75% minimum $Ca(OH)_2$)	<6%	–	Whitish	Powder

in a double beam Atomic Absorption Spectrometer (AAS) (AAnalyst 300 Perkin Elmer, USA) equipped with a deuterium lamp, background corrector, and a hollow cathode lamp. The equipment was operated at 12 psi of dry air, 70 psi of acetylene, a 422.7 nm flame, a 10 mA lamp current, and a 0.7 nm slit width.

Ion Chromatography

Ion Chromatography (Chromatography Ionex DIONEX, Ion Pac AS16 column, and gradient pump GS50, USA) was used for analyses in parts-per-million (ppm) of fluoride anions.

Inductively Coupled Plasma-Mass Spectrometry (ICP-MS)

Quantitative analyses of the samples were made with a Thermo Series X2 ICP Mass Spectrometry System (Thermo Fisher Scientific, USA) equipped with Standard Sample Introduction System.

Fourier Transform Infrared (FT-IR)

FTIR Spectra of the samples were recorded in a Bruker Vector 33 spectrophotometer, according to diffuse reflectance technique [24].

Micro Raman spectrometry

The Raman spectra were recorded using a LabRam II micro-Raman spectrometer (Dilor, France). The 632.8 nm radiation from a helium–neon laser was used for excitation. The spectral resolution was 8 cm^{-1} and the band positions were accurate to ± 1 cm^{-1}. Neutral density filters were used to avoid sample damage.

Results and discussion

X-ray diffraction

Figure 1 shows the X-ray diffraction pattern of SA1, that consists primarily of cubic crystals, isometric system-hexoctaedral class of calcium oxide (CaO), as well as trigonal system-hexagonal scalenohedral class, crystals of portlandite ($Ca(OH)_2$) identified according to card 44–1481 from International Center for Diffraction Data (ICDD). Furthermore, the sample contains trigonal system-hexagonal trapezohedral class, quartz crystalline structure (SiO_4), in addition to trigonal system hexagonal scalenohedral class calcite crystalline structure ($CaCO_3$) (card 05–0586 ICDD), and monoclinic system prismatic class larnite crystals (Ca_2SiO) were observed. The quartz present in the X-ray diffraction pattern does not have any structural transformation during the calcination process as a result of the fusion temperature, which is around 2,000 °C. The presence of portlandite is related to the immediate reaction between calcium oxide and the moisture content of the environment.

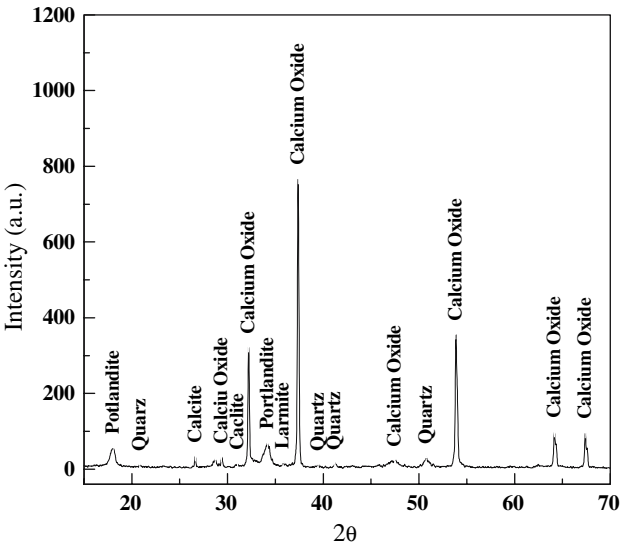

Fig. 1 X-ray diffraction patterns of SA1 showing the crystalline phases of calcium oxide, portlandite, quartz, and larnite

Figure 2 shows the X-ray diffraction pattern of SA2, and validates the physico-chemical and mineralogical changes in lime processing. The sample was a trigonal system, hexagonal; i.e., scalenohedral class crystals of portlandite ($Ca(OH)_2$). In addition, a trigonal system, hexagonal-scalenohedral class calcite crystals ($CaCO_3$) were detected,

along with a small presence of other crystals such as: trigonal system-hexagonal-trapezohedral class quartz crystals (SiO_2) (card 46-1045 ICDD) and monoclinic calcium silicate crystals ($Ca_2(SiO_4)$ (card 86-0398 ICDD)). An important point in this X-ray diffraction data is the presence of orthorhombic anhydrite crystals ($CaSO_4$)(card 37-1496 ICDD) marked in Fig. 2 with dash lines, revealing S traces in the SA2 sample but not in SA1, which is calcined with fuel oil (Fig. 1). The potential contamination could be present in any manufacturing method which uses a fuel oil or alternative heavy fuels. The origin of this phase can be explained by the exposure to polluted water, because the X-ray analysis of CaO did not show the existence of S compounds. SA2 had siliceous content in addition to the main component portlandite, which is the focal component of the lime-based products, while calcium silicate is the other predominant active component.

LV-SEM

Figure 3a and b show the SEM images of SA1 and SA2 taken at 5,000× and 20,000× respectively. According to these figures, the particle size distribution in the case of CaO is in the range of microns, while in the case of $Ca(OH)_2$, is in the range of sub-microns particles. CaO is a dynamic material, which immediately starts a chemical reaction with the atmospheric humidity, forming $Ca(OH)_2$. The activity of the CaO decays in a short time, and for this reason it is considered unstable. In addition, its caustic condition and violent reaction with water to generate a great amount of heat can cause sudden and unpredictable spitting. Such a process could be harmful to manage by unqualified people. This is the cause for the preference of the $Ca(OH)_2$ form.

In Fig. 3b most of the particles appear to be under 1 μm, but there is a broad range of sizes. Preliminary studies using Dynamic Light Scattering showed that the mean diameter is 6.643 μm and there are particles about 0.715 μm. The $Ca(OH)_2$ starts reacting immediately with the CO_2 from the atmosphere, forming $CaCO_3$, the most stable form of the analyzed calcium compounds. This produces the $Ca(OH)_2$ decay, meaning that the reactivity is a function of the $Ca(OH)_2$ age, along with the $Ca(OH)_2$ purity, which are important factors for the optimal calcium ion diffusion during the nixtamalization process.

Table 2 shows the content of elements detectable by electron dispersive scanning (EDS) using a semi-quantitative analysis in a random micro-region of SA1 and SA2. The elements found according to their weight percentage were Ca, O, C, Cu, Zn, and Fe. From the results, neither additional heavy metals nor other dangerous substances

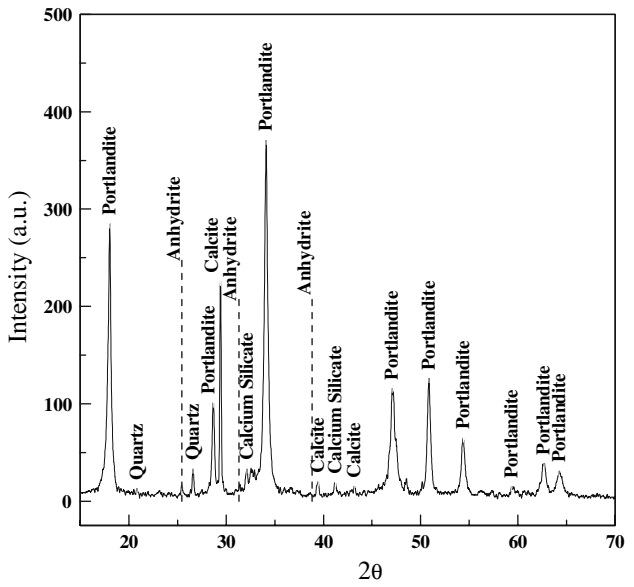

Fig. 2 X-ray diffraction patterns of SA″ showing the crystalline phases of portlandite, calcite, quartz, calcium silicate, and anhydrite which is marked by the dash lines

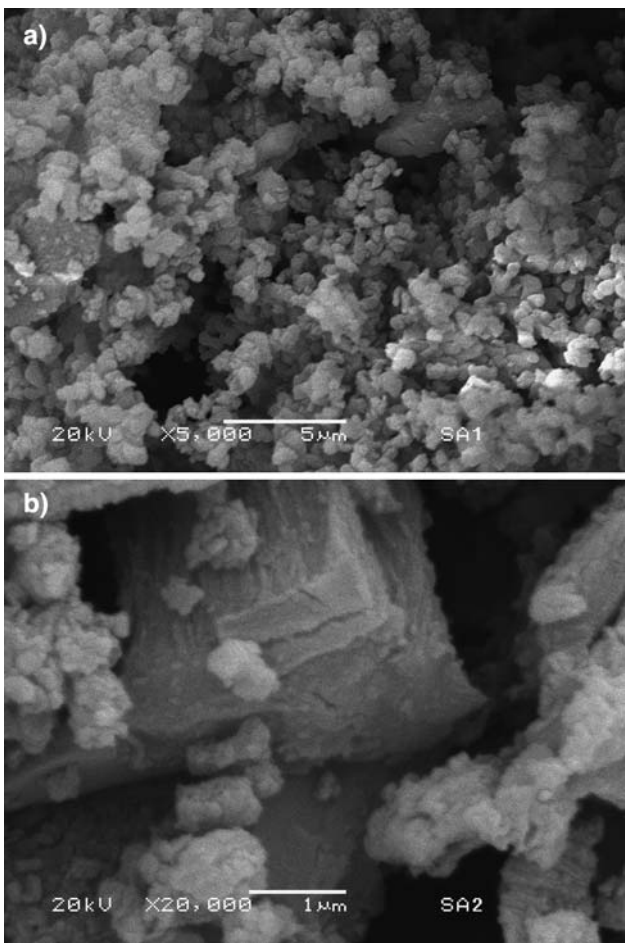

Fig. 3 (**a**) and (**b**) SEM micrographs of CaO (SA1) and $Ca(OH)_2$ (SA2)

Table 2 SEM semi-quantitative analysis by EDS

Sample	% Weight									
	C	O	Al	Si	K	Ca	Fe	Cu	Zn	Total
SA1	5.43	42.68	–	–	–	45.79	–	3.38	2.72	100
SA2	5.93	43.11	–	–	–	43.88	1.42	3.20	2.45	100

The table lists the elements in major, minor, and trace quantities

were detected in the analyzed micro-regions of the samples with this technique.

Atomic Absorption Spectroscopy (AAS) and Ion Chromatography (IC)

Table 3 shows the quantitative analyses of SA1 and SA2 by AAS, to measure Ca, Mg, K, and Pb; and Ion Chromatography to determine the F content. The potential of Pb contamination could be present in any manufacturing procedure which uses a direct flame process. Some coals used for direct-firing may cause contamination of products with H_2S and SO_2. Direct firing with petroleum coke may cause contamination with V, H_2S, SO_2 and various thiosulfates. In spite of this concern, the Pb content in the samples was below AAS quantification limit (0.5 mg/kg). Compared with the acceptable limit (8 mg/kg) by the Food Chemicals Codex standards, CaO and $Ca(OH)_2$ must contain no more Pb than 10 mg/kg. The Pb contents in SA1 and SA2 were satisfactory for safe human consumption. Additionally, the detection by IC was used in order to determine the accurate concentration of fluorine anion in solution. Similarly, compared with the acceptable limit (40 mg/kg), the fluorine content in both samples was adequate for safe human consumption. No pollutants were detected in dangerous quantities from the gases added to CaO from fossil fuel combustion and later hydratation with uncontrolled quality of water during calcium hydroxide production process. Within the general working range, the minimum detectable concentrations by AAS were 0.05 mg/kg.

Inductively Coupled Plasma-Mass Spectrometry (ICP-MS)

Table 4 summarizes the results of dangerous element contents from the ICP-MS analyses. After revision of the Norma Oficial Mexicana NOM 187-SSA1/SCSI-2002 [25], it is the same as Food Chemicals Codex—FDA regulations [26], FAO Codex Alimentarius [27], and European Union Food list of approved additives [17]. The contents of Pb, F, and As were below the respective limits considered dangerous to health. Additionally, the content of other elements not cited in the regulations were included. Pb quantification was established exactly by this technique, contrasting with the result obtained through AAS, where the determination was noted as just under the quantification limit. The variation of V content (not listed in regulatory outlines) between samples SA1 and SA2 was relevant, with less content in SA1 before the addition of water for hydratation process. Because some fuel oils include considerable amounts of V and CaO is usually produced by direct firing with heavy fuel oil, this is a possible contamination source. In such cases, an examination to determine the existence of V is appropriate.

FTIR

In Fig. 4a the observed absorption bands of SA1 FT-IR pattern and their respective assignments are reported and simultaneously under-imposed with the standard calcium oxide spectra (Fermont—CAS 1305-78-8) in dotted lines. The two has similar shoulders, implying that there were no relevant impurities. According to Farcas and Touzé [28], the strong band at 3,643 cm^{-1} corresponds to the O–H stretching vibration, unique to water. The presence of this band is evidence for the existence of liquid water in the sample. The wide shoulder at the 1,417 cm^{-1} band matches the C–O vibration, similar to shoulder at the 866 cm^{-1}, which corresponds to C–O vibration. The band at 511 cm^{-1} was due to Ca–O symmetric vibration. No pollutants were detected from these spectra.

In Fig. 4b, absorption bands of SA2 FTIR, the shoulder at 3,871 cm^{-1} was attributed to vibrations of O-H group. In a similar way the strong band at 3,643 cm^{-1} was assigned to stretching vibration of O–H bond. Bands at 1,427 cm^{-1} and 875 cm^{-1} were identified as C–O stretching vibrations. There is a relevant shoulder at 1,126 cm^{-1} related to S–O vibration, because it confirms the presence of S, previously discussed in the DRX section. The shoulder at 457 cm^{-1} was attributed to symmetric vibrations of Ca–O. The simultaneously under-imposed of standard calcium hydroxide spectra (Fermont 98.6%) in dotted lines has similar shoulders as the spectra of SA2, validating the material as calcium hydroxide.

Table 3 Quantification by AAS (Ca, Mg, K, Pb), and by Ion Chromatography (F)

Sample	Ca mg/kg	Mg mg/kg	K mg/kg	Na mg/kg	Pb mg/kg	F mg/ kg
SA1	1,394	9.8	1.0	2.5	<q.l.	<q.l.
SA2	1,274	16.0	1.2	2.7	<q.l.	<q.l.
Quantification limit	0.5	0.5	0.1	0.5	0.5	0.5

Table 4 Quantification by ICP-MS

Sample	Concentration (mg kg^{-1})											
	Li	Be	V	Cr	Co	Ni	Cu	As	Se	Cd	Tl	Pb
SA1	0.0087	0.0	1.9068	0.1066	0.0686	1.4785	0.2742	0.0290	0.0	0.0	0.0	0.0012
SA2	0.3401	0.0	4.3403	0.2150	0.0884	1.1589	0.1932	0.0849	0.0	0.0	0.0	0.0527

Lead content was established

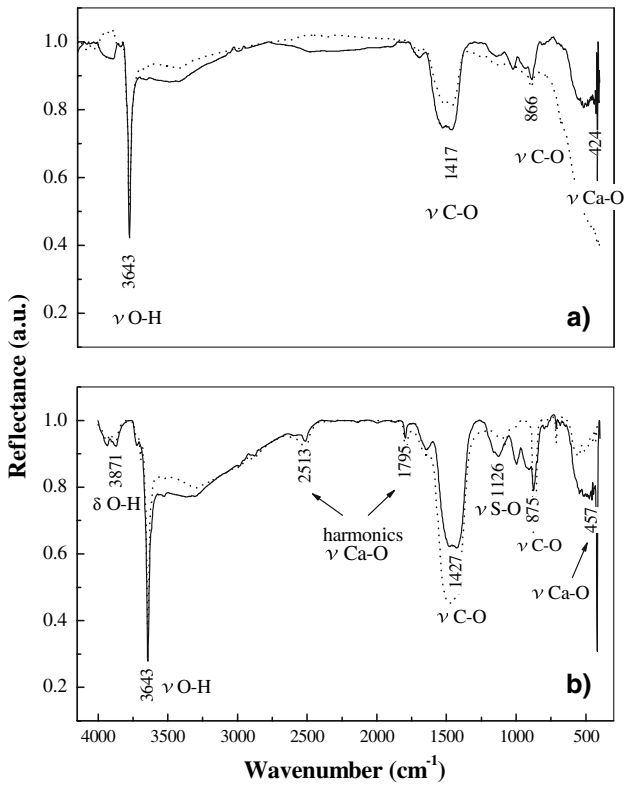

Fig. 4 (**a**) FTIR spectra. Solid line shows SA1 pattern; dotted line shows standard of calcium oxide standard spectra (Fermont—CAS 1305-78-8) (**b**) FTIR spectra. Solid line shows SA2 pattern; dotted line shows spectra of calcium hydroxide standard spectra (Fermont 98.6%)

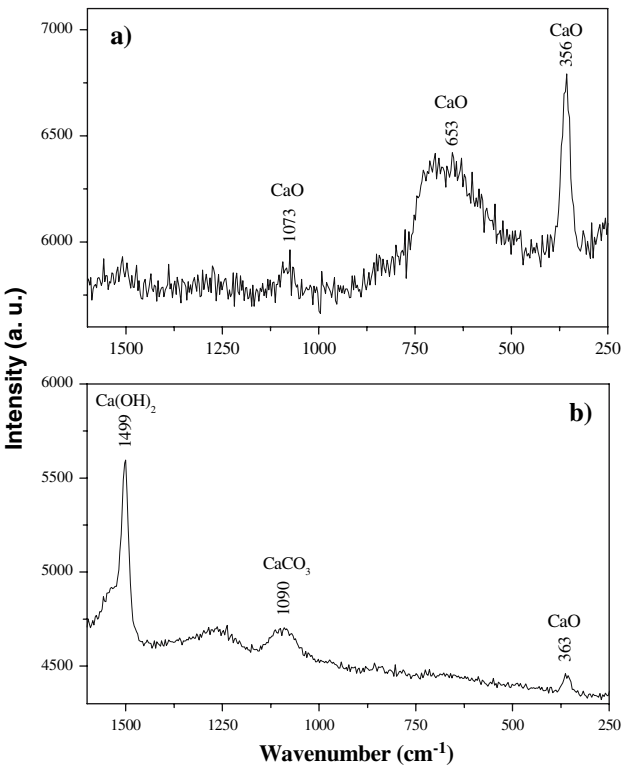

Fig. 5 (**a**) Raman patterns showed vibrational frequency shifts of calcium oxide. (**b**) Raman patterns showed vibrational frequency shifts of calcium hydroxide

Raman

Raman is an effective technique to determine the presence of oxides species. Raman spectra of SA1 and SA2 are shown in Fig. 5a and b respectively. The Raman spectra of SA1 show a high fluorescence background. In spite of this fact, the carbonate anion symmetric stretching band at 1,073 cm^{-1} is clearly noticed. The persistence of the Raman signal observed in SA1 can be explained by considering its higher content in Ca^{2+} ion arising from the corresponding carbonates which decomposed at high temperature during raw material calcination, giving rise to highly reactive calcium oxide. According to Edwards et al. [29] the spectra suggests that the peaks at 366, 653, and

1,073 cm^{-1} bands are a function of calcium oxide content. In addition, the spectra could be divided in three regions: the first region of low frequency (250–700 cm^{-1}); the second region of medium frequency (700–850 cm^{-1}), and the third region of high-frequency (850–1,300 cm^{-1}). The bands at 653 cm^{-1} and 356 cm^{-1} are a function of Ca–O bonds. In SA2, the band for calcium carbonate is at 1,090 cm^{-1}, and the band at 1,499 cm^{-1} arises from $CaCO_3$ bonds. The Raman spectra in both samples, SA1 and SA2, reveal no additional information about contamination considered a health hazard. According to FDA, $Ca(OH)_2$ as a food additive is specifically permitted as optional ingredient in a standardized food.

Conclusions

A series of measurements were made with the X-ray diffraction, inductively coupled plasma-mass spectrometry, atomic absorption spectroscopy, Fourier transform-infrared, and Raman spectroscopy to study calcium oxide and calcium hydroxide consumed in México and Central America as a food additive.

According to the results, Li, Be, V, Cr, Co, Ni, Cu, As, Se, Cd, Tl, Pb, as well as F in the analyzed samples meet the acceptable limits for safe human consumption. The most important issue is related to the introduced pollutants: V, F, Pb, and As. The samples analyzed in this work were considered safe for human consumption. Lime should be analyzed prior to their use as a food additive.

Acknowledgments This work was made possible with the technical assistance by Carolina Muñoz, Alicia del Real, Ofelia Pérez, Genoveva Hernández, and Francisco Rodríguez. The support from "Consejo del Sistema Nacional de Educación Tecnológica" and the "Asociación Nacional de Fabricantes de Cal" is highly appreciated.

References

1. C.B.E. Nordin, Nutrition **13**(7–8), 664 (1997)
2. M.L. Power, R.P. Heaney, H.J. Kalkwarf et al., Am. J. Obstet. Gynecol. **181**(6), 1560 (1999)
3. A. Flynn, Proc. Nutr. Soc. **62**, 851 (2003)
4. A. Flynn, A.K. Cashman, *Mineral Fortification of Foods*. (Leatherhead Food, UK, 1999)
5. E. Renner, M. Hermes, H. Stracke, Int. Dairy J. **8**, 759 (1998)
6. A. Prentice, Proc. Nutr. Soc. **56**, 357 (1997)
7. *Optimal Calcium Intake*. J. Am. Med. Assoc. **272**, 1942 (1994)
8. *Dietary reference intakes, Institute of Medicine* (National Academy Press, USA, 1997)
9. S.O. Serna-Saldivar, L.W. Rooney, L.W. Greene, Cereal Chem. **68**, 555 (1991)
10. S.O. Serna Saldivar, M.H. Gomez, H.D. Almeida Domínguez et al., Cereal Chem. **70**, 762 (1993)
11. M.E. Rodríguez, J.M. Yánez-Limón, A. Cruz-Orea et al., Z. Lebensm. Unsters. Forsch. **201**, 236 (1995)
12. M.E. Rodríguez, J.M. Yánez-Limón, J.J. Alvarado et al., Cereal Chem. **73**, 593 (1996)
13. L.W. Rooney, R.D. Waniska, C.M. McDonough et al., *Encyclopedia of Grain Science* (Elsevier, UK, 2004)
14. R. Bressani, N.S. Scrimshaw, J. Agric. Food Chem. **6**, 774 (1958)
15. R. Bressani, R. Paz y Paz, N.S. Scrimshaw, J. Agric. Food Chem. **6**, 770 (1958)
16. A. Cortés-Gómez, E. San Martín-Martínez, F. Martínez-Bustos et al., J. Food Eng. **66**, 273 (2005)
17. *List of current European Union approved additives and their E Numbers* (Food Standards Agency, E.U., 2002)
18. *Listing of specific substances affirmed as generally recognized as safe* (Title 21-Chapter I FDA, USA, 1977)
19. J.L. Fernández-Muñoz, M.E. Rodríguez, R.C. Pless et al., Cereal Chem. **79**, 162 (2002)
20. J.L. Fernandez-Muñoz, I. Rojas-Molina, M.L. Gonzalez-Davalos et al., Cereal Chem. **81**, 65 (2004)
21. J. Figueroa-Cárdenas, M.G. Acero-Godínez, T. Quezada-Tristán et al., Nutr. Res. **25**, 711 (2005)
22. *Estadística de producción nacional de hidróxido de calcio* (Asociación Nacional de Fabricantes de Cal, A.C., México, 2007)
23. *Official Method 968.08* (Association of Official Analytical Chemists, USA, 1998)
24. B.C. Smith, *Fundamentals of Fourier Transform Infrared Spectroscopy*, (CRC Press, USA, 1996)
25. *Norma Oficial Mexicana NOM 187-SSA1/SCSI*-(2002) (Diario Oficial de la Federación, México, 18 ago. 2003)
26. *FDA Code of Federal Regulations* (Title 21 vol. 3, USA, 2006)
27. *Codex Alimentarius* (Metals and arsenic specifications revised at the 59th JECFA, 2002)
28. F. Farcas, Ph. Touzé, Bulletin des LPC **230**, 77 (2001)
29. H.G.M. Edwards, S.E. Jorge-Villar, J. Jehlicka et al., Spectrochimica Acta **61**(10), 2273 (2005)